Rapid Communications

Neutrino self-interactions and double beta decay

Frank F. Deppisch,[1] Lukas Graf,[2] Werner Rodejohann,[2] and Xun-Jie Xu[2]

[1]*Department of Physics and Astronomy, University College London, Gower Street, London WC1E 6BT, United Kingdom*

[2]*Max-Planck-Institut für Kernphysik, Postfach 103980, D-69029 Heidelberg, Germany*

(Received 4 May 2020; accepted 19 August 2020; published 1 September 2020)

Neutrino self-interactions (νSI) beyond the Standard Model are an attractive possibility to soften cosmological constraints on neutrino properties and also to explain the tension in late and early time measurements of the Hubble expansion rate. The required strength of νSI to explain the 4σ Hubble tension is in terms of a pointlike effective four-fermion coupling that can be as high as $10^9 G_F$, where G_F is the Fermi constant. In this work, we show that such strong νSI can cause significant effects in two-neutrino double beta decay, leading to an observable enhancement of decay rates and to spectrum distortions. We analyze self-interactions via an effective operator as well as when mediated by a light scalar. Data from observed two-neutrino double beta decay are used to constrain νSI, which rules out the regime around $10^9 G_F$.

DOI: 10.1103/PhysRevD.102.051701

I. INTRODUCTION

The discrepancy between cosmic microwave background (CMB) and local measurements of the Hubble constant, known as the Hubble tension, has grown to about 4σ [1–5]. If indeed a physical fact, it would imply that nonstandard particle physics or cosmology is required. Introducing a neutrino self-interaction (νSI), i.e., a four-neutrino contact interaction, to inhibit neutrino free-streaming in the early Universe can resolve the Hubble tension. The required strength of νSI needs to be much larger than the Fermi effective interactions predicted in the Standard Model (SM) [6–10]. Writing the interaction as $G_S(\nu\nu)(\nu\nu)$,[1] there are two regimes for the coupling G_S: a strongly interacting regime with $G_S = 3.83^{+1.22}_{-0.54} \times 10^9\ G_F$ and a moderately interacting regime with $1.3 \times 10^6 < G_S/G_F < 1.1 \times 10^8$ [9].

The required strong νSI have drawn considerable attention [11–23], but in general they are difficult to probe in laboratory experiments due to the absence of electrons or quarks involved. Assuming that νSI are mediated by new light bosons, existing constraints come from big bang nucleosynthesis [12,24,25], pion/kaon decay [26–28], Z invisible decay [29,30], LHC searches [31], and supernova neutrinos [16–19]. There are currently no direct constraints on the νSI operator without any assumption on its origin.

In this paper, we propose to search for νSI in double beta decay experiments.[2] These experiments search for the lepton number violating, and thus SM-forbidden, neutrinoless double beta decay ($0\nu\beta\beta$) [33,34]. The standard diagram of this process is the exchange of a massive Majorana neutrino; see Fig. 1 (left). As part of this effort, the SM-allowed two-neutrino double beta ($2\nu\beta\beta$) decay is measured with increasing precision and may itself be used to probe physics beyond the Standard Model [35]. In the presence of νSI, two neutrinos can be emitted via the effective νSI operator; see Fig. 1 (right). The final state of this νSI-induced double beta ($2\nu_{\rm SI}\beta\beta$) decay is identical to that of $2\nu\beta\beta$ decay.

In previous studies of double beta decay, indirect constraints on νSI mediated by light scalars were obtained [36–43]. It was assumed that the scalar is emitted in the decay, hence is lighter than the Q-value of double beta decay. For a scalar particle ϕ that couples with strength g_ϕ to two electron neutrinos, one finds from searches for so-called Majoron emitting double beta decays that $g_\phi \lesssim 10^{-4}$–10^{-5} [38,39]. Taking $m_\phi = 1$ MeV, this bound on the Yukawa coupling corresponds to $G_S \lesssim (10\text{–}10^3) G_F$. If νSI are not mediated by light scalars or the scalar mass is larger than the Q-value, this bound does not apply. In this case, the effect of νSI operators on double beta decay becomes more important, which we will investigate here.

II. νSI-INDUCED DOUBLE BETA DECAY

In the standard $0\nu\beta\beta$ mechanism, two neutrinos produced in double beta decay annihilate due to a Majorana mass term, leaving only electrons in the leptonic final

[1]Here we adopt the Weyl spinor notation, with ν being a two-component spinor, and the combination $(\nu\nu)$ is a scalar product.

[2]For future prospects in beta decay experiments, see Ref. [32].

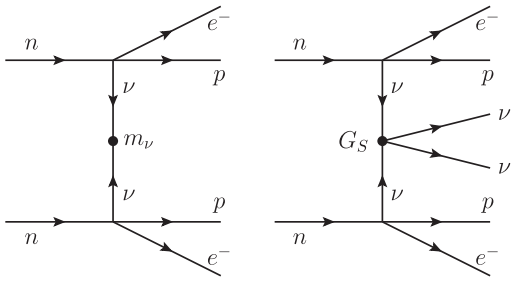

FIG. 1. Left: Neutrinoless double beta decay via Majorana neutrino exchange. Right: νSI-induced double beta decay.

states, as shown in Fig. 1 (left). Under the presence of νSI operators,

$$\mathcal{L}^{\rm LNC}_{\nu\rm SI} = G_S(\nu_e\nu_e)(\bar{\nu}_\alpha\bar{\nu}_\beta), \quad \text{or}$$
$$\mathcal{L}^{\rm LNV}_{\nu\rm SI} = G_S(\nu_e\nu_e)(\nu_\alpha\nu_\beta), \tag{1}$$

where $\alpha,\beta = e,\ \mu,\ \tau$ are flavor indices, and Fig. 1 (right) implies that the two electron-antineutrinos ($\bar{\nu}_e$) generated by neutron decay can take part in the νSI interaction and convert in the $2\nu_{\rm SI}\beta\beta$ process to $\nu_\alpha\nu_\beta$ or $\bar{\nu}_\alpha\bar{\nu}_\beta$. Note that both the lepton number conserving (LNC) and violating (LNV) interactions in Eq. (1) can lead to $2\nu_{\rm SI}\beta\beta$.

Assuming that the momenta of leptonic final states are negligible compared to the momenta of the neutrino propagators [the typical values of the former and the latter are of order $Q = \mathcal{O}(1)$ MeV and $p_F = \mathcal{O}(100)$ MeV, respectively], the two processes in Fig. 1 share the same nuclear matrix elements (NMEs). Consequently, we can compute the decay rate of $2\nu_{\rm SI}\beta\beta$ using the NME of $0\nu\beta\beta$,

$$\Gamma_{\nu\rm SI} = \left|\frac{G_S m_e}{2R}\right|^2 \mathcal{G}_{\nu\rm SI}|\mathcal{M}_{0\nu}|^2. \tag{2}$$

Here m_e denotes the electron mass, R is the radius of the nucleus, $\mathcal{M}_{0\nu}$ is the $0\nu\beta\beta$ NME, and $\mathcal{G}_{\nu\rm SI}$ is the $2\nu_{\rm SI}\beta\beta$ phase space factor (derived in the Supplemental Material [44]), which reads

$$\mathcal{G}_{\nu\rm SI} = \frac{2c_{\nu\rm SI}}{15}\int dp_1 dp_2 p_1^2 p_2^2 (Q - T_{12})^5 F^2(p_1,p_2), \tag{3}$$

where p_1 and p_2 are the momenta of the two electrons. The Q-value is given in Table I for various isotopes and $F^2(p_1,p_2)$ stands for the Fermi function correction caused by the Coulomb potential of the nucleus. Finally, $T_{12} = E_1 + E_2 - 2m_e$ is the total kinetic energy of both electrons, implicitly depending on p_1 and p_2, and neutrino masses in the final state have been neglected. The constant $c_{\nu\rm SI}$ is determined by $c_{\nu\rm SI} = (G_F^4\cos^4\theta_C)/(256\pi^9 m_e^2)$, where θ_C denotes the Cabibbo angle. Note that the electron mass m_e and nuclear radius R are included in Eq. (2) so that the normalization of the NME and phase space factor conforms with that adopted in the literature.

Using Eqs. (2) and (3), it is straightforward to compute $\Gamma_{\nu\rm SI}$. It should be noted, however, that the electron spectrum of $2\nu_{\rm SI}\beta\beta$ is very similar to that of $2\nu\beta\beta$ decay. Potential differences will be discussed later. Here let us first focus on the total decay rate. The total rate $\Gamma_{2\nu}$ of $2\nu\beta\beta$ decay has been measured precisely for many isotopes. For example, the $2\nu\beta\beta$ rate of ^{136}Xe has been measured to a 3% level [52]. Nonetheless, there remains a considerable uncertainty in the theoretical prediction of the $2\nu\beta\beta$ decay rate arising from the NMEs. Unresolved issues such as the quenching of the effective nuclear axial coupling g_A in $0\nu\beta\beta$ decay likely provide a major error source. We proceed with a conservative requirement that the $2\nu_{\rm SI}\beta\beta$ rate is less than the $2\nu\beta\beta$ rate,

$$\Gamma_{\nu\rm SI}/\Gamma^{\rm ex}_{2\nu} < 1, \tag{4}$$

where $\Gamma^{\rm ex}_{2\nu}$ stands for the experimentally measured value of $2\nu\beta\beta$.

Taking the best-fit value of $G_S = 3.83\times10^9 G_F$ of the strongly interacting regime and the interacting boson model (IBM-2) NMEs [46], we compute the decay rate $\Gamma_{\nu\rm SI}$ (assuming the unquenched value $g_A = 1.269$ in the calculation of the NMEs) and compare it with $\Gamma^{\rm ex}_{2\nu}$ in Table I. By requiring $\Gamma_{\nu\rm SI}/\Gamma^{\rm ex}_{2\nu} < 1$, we obtain the corresponding constraints on G_S, which is presented in Fig. 2. Here, we also

TABLE I. Estimate of $2\nu_{\rm SI}\beta\beta$ decay rates for several isotopes. Here, Q is the corresponding Q-value, $T^{2\nu}_{1/2}$ represents the experimental $2\nu\beta\beta$ decay half-lives adopted from Ref. [45] that can be translated to the experimental $2\nu\beta\beta$ decay rates using $\Gamma^{\rm ex}_{2\nu} = \log 2/T^{2\nu}_{1/2}$ and $\Gamma_{\nu\rm SI}$ denotes the theoretical prediction for the $2\nu_{\rm SI}\beta\beta$ decay rates computed from Eq. (2), assuming $G_S = 3.83\times10^9 G_F$. Bounds on G_S obtained according to Eq. (4) are presented in the last row. Nuclear matrix element values from IBM-2 [46] are used to obtain the values in this table.

	^{48}Ca	^{76}Ge	^{136}Xe	^{100}Mo	^{128}Te	^{130}Te
Q/MeV	4.263 [47]	2.039 [48]	2.458 [49]	3.034 [48]	0.8659 [50]	2.527 [51]
$T^{2\nu}_{1/2}$/year	5.30×10^{19}	1.88×10^{21}	2.17×10^{21}	6.88×10^{18}	2.25×10^{24}	7.91×10^{20}
$(\Gamma_{\nu\rm SI})^{-1}$/year	2.52×10^{18}	1.42×10^{20}	1.55×10^{19}	2.94×10^{18}	4.04×10^{22}	9.08×10^{18}
$\Gamma_{\nu\rm SI}/\Gamma^{\rm ex}_{2\nu}$	78.6	49.5	528	8.76	209	326
$G_S/G_F <$	4.32×10^8	5.44×10^8	1.67×10^8	1.29×10^9	2.65×10^8	2.12×10^8

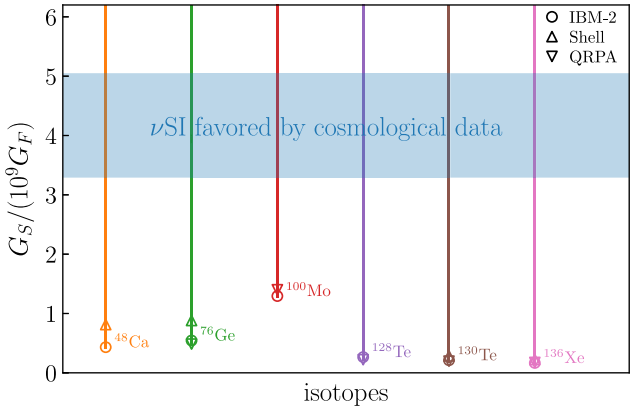

FIG. 2. Upper limit on the νSI coupling G_S from $2\nu\beta\beta$ decay data for several isotopes and three different NME calculations as indicated. The blue band corresponds to the strongly interacting regime $G_S = 3.83^{+1.22}_{-0.54} \times 10^9 G_F$ favored by cosmological data, which here is excluded by observations of $2\nu\beta\beta$ of various isotopes.

use NME values computed in the interacting shell model (Shell) [53] and quasiparticle random phase approximation (QRPA) model [54]; the corresponding limits on G_S are shown in Fig. 2, indicating the uncertainty arising from nuclear theory uncertainties. As one can see, the strongly interacting regime for G_S favored by the cosmological data causes $\Gamma_{\nu\mathrm{SI}}/\Gamma^{\mathrm{ex}}_{2\nu} > 1$ for all the isotopes listed in Table I. For some isotopes, $\Gamma_{\nu\mathrm{SI}}$ can be even 1 or 2 orders of magnitude higher than $\Gamma^{\mathrm{ex}}_{2\nu}$. Even including the theoretical NME uncertainties, most isotopes can fully exclude the cosmologically favored strongly interacting regime band, given the premise that two ν_e are involved in the νSI.

III. ENERGY AND ANGULAR DISTRIBUTIONS

We now consider possible distortions of the electron energy and angular distributions arising from the νSI-induced contribution. For an exact contact interaction of four neutrinos and neglecting final state lepton momenta, one can show that the electron spectra of $2\nu_{\mathrm{SI}}\beta\beta$ decay are the same as that of $2\nu\beta\beta$ decay; see the Supplemental Material [44]. However, considering that the νSI operator may be generated by light mediators, the corresponding energy dependence of G_S can cause observable spectral distortions, as we shall discuss below. We should mention here that the spectral distortions depend on the underlying model for νSI, which currently still lacks comprehensive exploration. There are various possibilities to generate the νSI effective operator, as shown in Fig. 3, where both tree and one-loop level diagrams are illustrated.

At tree level, the νSI operator can be opened via either an s-channel (diagram I) or a t-channel (diagram II) scalar mediator. For vector mediators, most of the discussions

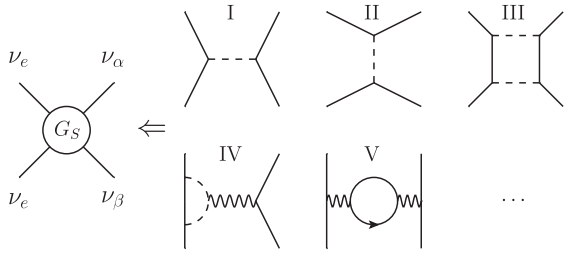

FIG. 3. νSI generation at tree and loop level. Here, scalar (vector) lines may also be replaced by vector (scalar) lines.

below apply as well.[3] For the s- and t-channel diagrams, G_S has the following energy dependence:

$$G_S = \frac{-m_\phi^2}{s - m_\phi^2} G_S^0 \quad (s\text{-channel}), \tag{5}$$

$$G_S = \frac{m_\phi^2}{t + m_\phi^2} G_S^0 \quad (t\text{-channel}), \tag{6}$$

where m_ϕ is the mediator mass and $s \equiv p^2$, $t \equiv -q^2$ with p and q being the momenta of the mediators in the tree diagrams. In the context of $2\nu_{\mathrm{SI}}\beta\beta$, they are of order $t \sim p_F^2$ and $s \lesssim Q^2$, respectively. The values of G_S at zero momentum transfer are denoted as $G_S^0 = g_\phi^2/m_\phi^2$, with the coupling g_ϕ between ϕ and the neutrinos. Note that in Eq. (5) we omit the small effect of the ϕ decay width.

At the one-loop level, the νSI operators can be generated e.g., by the box diagram in Fig. 3. The corresponding energy dependence of G_S is much more complicated than in the tree-level case. In general, it depends on both $s = p^2$ and $t = -q^2$. However, for most loop diagrams, there are no simple analytical expressions similar to Eqs. (5) and (6). For the box diagram, we can obtain a simple result assuming all the particles running in the loop have the same mass m_ϕ and that $s \ll t \ll m_\phi^2$. With these assumptions, following the calculation in Ref. [56], we get

$$G_S = G_S^0\left(1 - \frac{3}{10}\frac{t}{m_\phi^2} + \cdots\right). \tag{7}$$

Compared to Eq. (6), where the expansion in t yields $G_S = G_S^0(1 - t/m_\phi^2 + \cdots)$, the t/m_ϕ^2 term in Eq. (7) has a different coefficient but the same sign. In addition to the box diagram, other one-loop diagrams are also possible, as illustrated by diagrams IV and V in Fig. 3. Such diagrams can be roughly regarded as tree-level diagrams with energy-dependent couplings or mediator masses, which may cause more elusive effects in probing νSI in experiments of

[3]However, if the s-channel mediator is a vector boson, the process would be suppressed by the tiny neutrino masses due to the required chirality flipping [55].

different energy scales. Here we only mention these possibilities and refrain from further discussions[4].

Among the aforementioned possibilities, only the s-channel case in Eq. (5) can be analyzed without involving novel nuclear physics calculations. Other t-dependent scenarios necessarily involve integrals over q that are different from the one in $0\nu\beta\beta$ decay, which calls for a dedicated study in the future. Here we proceed only with the s-channel case, specifically for $m_\phi \gtrsim Q$. While the t-channel may also contribute in this regime, its effect is expected to be considerably smaller due to the large t suppression in the propagator. For G_S in Eq. (5), we have derived the $2\nu_{\rm SI}\beta\beta$ differential decay rate in the Supplemental Material [44] yielding the dependence,

$$\frac{d\Gamma_{\nu\rm SI}}{dp_1 dp_2 d\cos\theta_{12}} \propto |G_S^0|^2 p_1^2 p_2^2 F^2(p_1,p_2) \times I_s(T_{12})(1-\beta_1\beta_2\cos\theta_{12}). \quad (8)$$

Here, $\cos\theta_{12} = \mathbf{p}_1\cdot\mathbf{p}_2/(p_1p_2)$ with the angle $0 \le \theta_{12} \le \pi$ between the two emitted electrons and $\beta_i = p_i/E_i$ are the electron velocities. The effect of the s-channel mediating scalar is captured by the function,

$$I_s(T_{12}) = \frac{Q-T_{12}}{4(2\pi)^4}\left(\xi\frac{2+\cos\xi}{\sin\xi} - 3\right), \quad (9)$$

where $\xi = 2\arcsin((Q-T_{12})/m_\phi)$. It is a function of the total electron kinetic energy T_{12}, and as we will see it can cause distortions of both the energy and angular distributions of the electrons. In the limit $m_\phi \to \infty$, the effective operator is recovered, and the dependence approaches $I_s(T_{12}) \propto (Q-T_{12})^5$ yielding a phase space factor equivalent to $2\nu\beta\beta$ decay.

We first consider the energy distribution. All modern double beta decay experiments measure the differential decay rate $d\Gamma_{\nu\rm SI}/dT$ with respect to the total electron kinetic energy. This rate is computed by integrating over $\cos\theta_{12}$, p_1 and p_2 with the total kinetic energy $T = T_{12}$ fixed at a given value. As noted, in the limit $m_\phi \to \infty$, $d\Gamma_{\nu\rm SI}/dT$ will have the same energy distribution as that of $2\nu\beta\beta$ decay.

In Fig. 4 (left), we show the electron energy distributions of $2\nu_{\rm SI}\beta\beta$ and $2\nu\beta\beta$ decay for the isotope ^{100}Mo with an s-channel mediator mass $m_\phi = Q + 0.1m_e$, slightly above the kinematic threshold. For comparison, we also show a vertical line corresponding to $0\nu\beta\beta$ decay and the distribution for Majoron emission ($0\nu\beta\beta\phi$) taken from Ref. [42]. As can be seen in Fig. 4, the energy spectrum of $2\nu_{\rm SI}\beta\beta$ decay is shifted towards lower energies when compared to the $2\nu\beta\beta$ spectrum. The shift can be understood qualitatively. With increasing T the energy taken away by neutrinos is smaller, leading to a smaller value of s and hence a smaller value of the s-channel G_S. To determine the experimental sensitivity to such distortion, we have performed a simple χ^2-fit to the NEMO-3 data [58] as detailed in the Supplemental Material [44]. We find that for $\Gamma_{\nu\rm SI} = r^2\Gamma_{2\nu}$ with $r = 16\%$, the χ^2-value is changed by $\Delta\chi^2 = 9$ (3σ), which implies that if the spectral distortion is taken into account, the bound on G_S can be approximately improved by 1 order of magnitude. We emphasize that this applies for the specific mediator mass $m_\phi = Q + 0.1m_e$ and the sensitivity will decrease for larger masses.

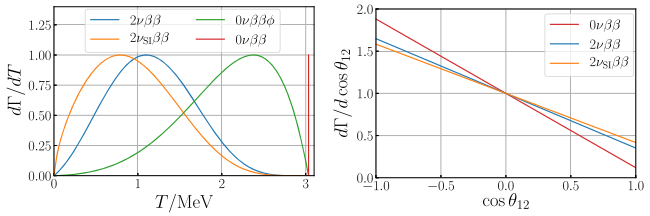

FIG. 4. Energy (left panel) and angular (right panel) distributions of $2\nu_{\rm SI}\beta\beta$, in comparison with other types of $\beta\beta$ decay. All spectra are normalized to 1 at the peaks (left) or at $\cos\theta_{12} = 0$ (right), so the figure is in arbitrary units.

In addition to the energy distribution, the angular distribution can also be measured in dedicated experiments such as NEMO-3 [58] and SuperNEMO [59]. From Eq. (8), the angular distribution of $2\nu_{\rm SI}\beta\beta$ decay is obtained by integrating out p_1 and p_2. The result takes the form,

$$\frac{d\Gamma_{\nu\rm SI}}{d\cos\theta_{12}} = \frac{\Gamma_{\nu\rm SI}}{2}(1 - k_\theta^{\nu\rm SI}\cos\theta_{12}), \quad (10)$$

where the angular correlation $k_\theta^{\nu\rm SI}$ can be computed according to Eq. (8). For $2\nu\beta\beta$ and $0\nu\beta\beta$ decay, the electron angular distributions take the same form as Eq. (10), but with different angular coefficients k_θ [59,60]. We refer to those as $k_\theta^{0\nu}$ and $k_\theta^{2\nu}$, respectively. For ^{100}Mo, the numerical values are $k_\theta^{\nu\rm SI} = 0.58$ (using again $m_\phi = Q + 0.1m_e$), $k_\theta^{2\nu} = 0.65$ and $k_\theta^{0\nu} = 0.88$. With these values, we show in Fig. 4 (right) the angular distributions of electrons for the three processes. Again, we have performed a χ^2-fit to the NEMO-3 data [58], and the result is $r < 29\%$ at 3σ confidence level. This indicates that the angular distribution is less sensitive than the energy distribution to distortions from $2\nu_{\rm SI}\beta\beta$. This is in fact interesting, as among the running and future experiments only one (SuperNEMO) has sensitivity on the angular distribution.

IV. CONCLUSION AND DISCUSSION

The search for $0\nu\beta\beta$ decay constitutes one of the most important aspects to determine the nature and properties of neutrinos. As we have demonstrated in Figs. 2 and 4, in the

[4]We note that νSI may also lead to significant corrections to the neutrino self-energy, which is not fully identical to the neutrino mass in $0\nu\beta\beta$ [57]. The effect is quite model-dependent and can be studied if a complete model of νSI has been constructed.

presence of νSI involving two ν_e, there can be significant effects not only on the total rates of $2\nu\beta\beta$ decay, but also on the spectrum shapes. If only the total rates are considered, we find that ^{136}Xe currently has the best sensitivity to νSI. The observed $2\nu\beta\beta$ rate implies $G_S < (0.17 - 0.22) \times 10^9 G_F$, which is significantly lower than the cosmologically favoured value $G_S = 3.83^{+1.22}_{-0.54} \times 10^9 G_F$ in the strongly interacting regime. However, one should note that this bound does not apply if only ν_μ and ν_τ participate in νSI.

Including spectral distortions could further improve the sensitivities. This is of interest when the particle that mediates the self-interactions has a mass that is larger than the available Q-value of the double beta decay. The distortions are caused by the energy dependence of the effective coupling G_S and hence are affected by the underlying models for νSI. In this work, we only consider an s-channel mediating scalar, which allows us to evade nuclear physics calculations and to quantitatively show spectral distortions of the energy and angular distributions. For other possibilities containing a t-channel dependence, very different spectral distortions could appear, which will be addressed when a more dedicated study involving nuclear physics calculations is carried out.

In our calculations, we neglected potential interference between the SM $2\nu\beta\beta$ and $2\nu_{\rm SI}\beta\beta$ processes, which in principle would be present if two electron antineutrinos are emitted in the νSI-mediated process. When the $2\nu\beta\beta$ rate can be theoretically determined precisely, interference term could be of significant importance—see the Supplemental Material [44].

In summary, our work shows that strong νSI favored by the cosmological data might have an impact on $2\nu\beta\beta$ decay experiments. Precision measurements of $2\nu\beta\beta$ decay spectra combined with more theoretical effort in computing NMEs have the potential of probing hidden interactions of neutrinos. Furthermore, it demonstrates the importance of having access to energy and angular distributions of electrons in double beta decay experiments.

ACKNOWLEDGMENTS

W. R. is supported by the DFG with Grant No. RO 2516/7-1 in the Heisenberg program. F. F. D. acknowledges support from the UK Science and Technology Facilities Council (STFC) via a Consolidated Grant (Reference ST/P00072X/1).

[1] A. G. Riess *et al.*, Astrophys. J. **826**, 56 (2016).
[2] T. Shanks, L. Hogarth, and N. Metcalfe, Mon. Not. R. Astron. Soc. **484**, L64 (2019).
[3] A. G. Riess, S. Casertano, D. Kenworthy, D. Scolnic, and L. Macri, arXiv:1810.03526.
[4] N. Aghanim *et al.* (Planck Collaboration), arXiv:1807.06209.
[5] A. G. Riess, S. Casertano, W. Yuan, L. M. Macri, and D. Scolnic, Astrophys. J. **876**, 85 (2019).
[6] F.-Y. Cyr-Racine and K. Sigurdson, Phys. Rev. D **90**, 123533 (2014).
[7] L. Lancaster, F.-Y. Cyr-Racine, L. Knox, and Z. Pan, J. Cosmol. Astropart. Phys. 07 (2017) 033.
[8] I. M. Oldengott, T. Tram, C. Rampf, and Y. Y. Y. Wong, J. Cosmol. Astropart. Phys. 11 (2017) 027.
[9] C. D. Kreisch, F.-Y. Cyr-Racine, and O. Dore, Phys. Rev. D **101**, 123505 (2020).
[10] M. Park, C. D. Kreisch, J. Dunkley, B. Hadzhiyska, and F.-Y. Cyr-Racine, Phys. Rev. D **100**, 063524 (2019).
[11] J. Hasenkamp, Phys. Rev. D **93**, 055033 (2016).
[12] G.-y. Huang, T. Ohlsson, and S. Zhou, Phys. Rev. D **97**, 075009 (2018).
[13] P. Bakhti, Y. Farzan, and M. Rajaee, Phys. Rev. D **99**, 055019 (2019).
[14] N. Blinov, K. J. Kelly, G. Z. Krnjaic, and S. D. McDermott, Phys. Rev. Lett. **123**, 191102 (2019).
[15] A. De Gouvea, M. Sen, W. Tangarife, and Y. Zhang, Phys. Rev. Lett. **124**, 081802 (2020).
[16] A. Das, A. Dighe, and M. Sen, J. Cosmol. Astropart. Phys. 05 (2017) 051.
[17] A. Dighe and M. Sen, Phys. Rev. D **97**, 043011 (2018).
[18] H. Ko *et al.*, J. Phys. Soc. Jpn. Conf. Proc. **31**, 011027 (2020).
[19] S. Shalgar, I. Tamborra, and M. Bustamante, arXiv:1912.09115.
[20] F. Forastieri, M. Lattanzi, and P. Natoli, Phys. Rev. D **100**, 103526 (2019).
[21] K.-F. Lyu, E. Stamou, and L.-T. Wang, arXiv:2004.10868.
[22] H.-J. He, Y.-Z. Ma, and J. Zheng, arXiv:2003.12057.
[23] M. Berbig, S. Jana, and A. Trautner, arXiv:2004.13039.
[24] C. Boehm, M. J. Dolan, and C. McCabe, J. Cosmol. Astropart. Phys. 12 (2012) 027.
[25] A. Kamada and H.-B. Yu, Phys. Rev. D **92**, 113004 (2015).
[26] V. D. Barger, W.-Y. Keung, and S. Pakvasa, Phys. Rev. D **25**, 907 (1982).
[27] A. P. Lessa and O. L. G. Peres, Phys. Rev. D **75**, 094001 (2007).
[28] P. S. Pasquini and O. L. G. Peres, Phys. Rev. D **93**, 053007 (2016); **93**, 079902(E) (2016).
[29] J. M. Berryman, A. De Gouvea, K. J. Kelly, and Y. Zhang, Phys. Rev. D **97**, 075030 (2018).
[30] V. Brdar, M. Lindner, S. Vogl, and X.-J. Xu, Phys. Rev. D **101**, 115001 (2020).
[31] A. de Gouvea, P. B. Dev, B. Dutta, T. Ghosh, T. Han, and Y. Zhang, J. High Energy Phys. 07 (2020) 142.

[32] G. Arcadi, J. Heeck, F. Heizmann, S. Mertens, F. S. Queiroz, W. Rodejohann, M. Slezak, and K. Valerius, J. High Energy Phys. 01 (2019) 206.
[33] F. F. Deppisch, M. Hirsch, and H. Pas, J. Phys. G **39**, 124007 (2012).
[34] M. J. Dolinski, A. W. P. Poon, and W. Rodejohann, Annu. Rev. Nucl. Part. Sci. **69**, 219 (2019).
[35] F. F. Deppisch, L. Graf, and F. Simkovic, arXiv:2003.11836.
[36] C. P. Burgess and J. M. Cline, Phys. Lett. B **298**, 141 (1993).
[37] C. P. Burgess and J. M. Cline, Phys. Rev. D **49**, 5925 (1994).
[38] A. Gando *et al.* (KamLAND-Zen Collaboration), Phys. Rev. C **86**, 021601 (2012).
[39] M. Agostini *et al.*, Eur. Phys. J. C **75**, 416 (2015).
[40] K. Blum, Y. Nir, and M. Shavit, Phys. Lett. B **785**, 354 (2018).
[41] R. Cepedello, F. F. Deppisch, L. Gonzalez, C. Hati, and M. Hirsch, Phys. Rev. Lett. **122**, 181801 (2019).
[42] T. Brune and H. Paes, Phys. Rev. D **99**, 096005 (2019).
[43] Y. Farzan, M. Lindner, W. Rodejohann, and X.-J. Xu, J. High Energy Phys. 05 (2018) 066.
[44] See Supplemental Material at http://link.aps.org/supplemental/10.1103/PhysRevD.102.051701 for calculation of the rate of νSI-mediated double beta decay.
[45] A. Barabash, AIP Conf. Proc. **2165**, 020002 (2019).
[46] J. Barea, J. Kotila, and F. Iachello, Phys. Rev. C **91**, 034304 (2015).
[47] M. Redshaw, G. Bollen, M. Brodeur, S. Bustabad, D. L. Lincoln, S. J. Novario, R. Ringle, and S. Schwarz, Phys. Rev. C **86**, 041306 (2012).
[48] S. Rahaman *et al.*, Phys. Lett. B **662**, 111 (2008).
[49] M. Redshaw, E. Wingfield, J. McDaniel, and E. G. Myers, Phys. Rev. Lett. **98**, 053003 (2007).
[50] N. D. Scielzo *et al.*, Phys. Rev. C **80**, 025501 (2009).
[51] S. Rahaman, V. V. Elomaa, T. Eronen, J. Hakala, A. Jokinen, A. Kankainen, J. Rissanen, J. Suhonen, C. Weber, and J. Aysto, Phys. Lett. B **703**, 412 (2011).
[52] J. B. Albert *et al.* (EXO-200 Collaboration), Phys. Rev. C **89**, 015502 (2014).
[53] J. Menendez, J. Phys. G **45**, 014003 (2018).
[54] J. Hyvarinen and J. Suhonen, Phys. Rev. C **91**, 024613 (2015).
[55] C. D. Carone, Phys. Lett. B **308**, 85 (1993).
[56] I. Bischer, W. Rodejohann, and X.-J. Xu, J. High Energy Phys. 10 (2018) 096.
[57] W. Rodejohann and X.-J. Xu, J. High Energy Phys. 11 (2019) 029.
[58] R. Arnold *et al.* (NEMO-3 Collaboration), Eur. Phys. J. C **79**, 440 (2019).
[59] R. Arnold *et al.* (SuperNEMO Collaboration), Eur. Phys. J. C **70**, 927 (2010).
[60] M. Doi, T. Kotani, and E. Takasugi, Prog. Theor. Phys. Suppl. **83**, 1 (1985).